Longitudinal Cross-Temporal Dynamics in Foreign Exchange via Bayesian Multifractal Analysis

Herwig Wendt
CNRS, Université de Toulouse
IRIT, Toulouse (FR)
herwig.wendt@irit.fr

Patrice Abry
CNRS, ENS de Lyon
Laboratoire de Physique, Lyon (FR)
patrice.abry@ens-lyon.fr

Yannick Malevergne
Université Paris 1 Panthéon-Sorbonne
PRISM Sorbonne, Paris (FR)
yannick.malevergne@univ-paris1.fr

Marc Senneret
Vivienne Investissement,
Research & Development, Lyon (FR)
msenneret@vivienne-im.com

Gérald Perrin
Vivienne Investissement,
Research & Development, Lyon (FR)
rgperrin@vivienne-im.com

Stéphane Jaffard
CNRS, Université Paris-Est,
LAMA, Créteil (FR)
stephane.jaffard@u-pec.fr

***Abstract*—Multifractal temporal dynamics in asset price time series are well documented stylized facts, that however remained univariate when multivariate (basket) properties are critical in financial applications, and for long enough samples only. This is due to a lack of theoretical and practical tools for multivariate multifractal analysis, and tools that can be used on short sample sizes. Recently, multivariate wavelet-leader multifractal analysis has been grounded theoretically and the corresponding Bayesian estimation framework developed. Elaborating on preliminary attempts, the Bayesian multivariate multifractal formalism is used to perform a short-term sliding window analysis of the cross-temporal dynamics for 17 years of exchange rates. Results suggest solid and reproducible organized bursts of co-volatilities with temporal dynamics mainly driven by the same clock worldwide.**

I. Introduction

Context. Accurately characterising the temporal and cross-temporal dynamics between asset prices has important implications for the financial industry, ranging from risk assessment to forecasting [1], [2]. It has been well-documented that financial time series are well modeled by multifractal dynamics [3]–[7]. Scalefree analyses remained however so far conducted in univariate settings for long enough sample size, mostly because of a lack in theoretically grounded practical tools that permit multivariate multifractal analyses of short duration samples. The questions of the existence and interest of multifractal cross temporal dynamics and of their evolution along time, using Bayesian multivariate multifractal analysis, constitute the heart of the present work. These are addressed by studying a basket of exchange rates, for 17 years.

Related work. After Mandelbrot's seminal works [3], numerous contributions supported scalefree temporal dynamics in financial time series, yet with no significant information in autocorrelation functions. This called for multifractal analysis for a richer characterisation of temporal dynamics beyond second-order statistics, that mostly converged toward modeling financial time series as subordinated Brownian motions, $B(A(t))$, where the random process $A(t)$ has multifractal properties that can be understood as modulating the course of time and thus controlling volatility burstiness [5]–[7]. These analyses remained however so far mostly conducted in univariate settings only (except in [7]) and for long enough sample size, by lack of theoretical multivariate multifractal theory and because of difficulties in multifractal parameter estimation. Elaborating on [8], a wavelet leader based multivariate multifractal theory was recently devised [9], [10]. Recently applied to a large size sample of a basket of exchange rate time series, it showed rich multifractal cross-temporal dynamics, with the joint occurrence of local transient structures in co-organized spatial patterns, and thus calling for further investigations [11]. In the same time frame, Bayesian estimation frameworks, first univariate [12] and then multivariate [13], [14] were devised, that permit the analysis of short sample size by improving estimation performance compared to classical linear regressions commonly used in multifractal analysis. Combining these recent advances paves the way for short time sliding window longitudinal multivariate multifractal analyses, the core contribution of the present work.

Goals, contributions and outline. The goal of this work is to perform a longitudinal study of the foreign exchange (forex) market, along 17 years (2005-2021), of the joint cross temporal dynamics of six major currency exchange rates, sampled at intraday high frequency, using the recently proposed wavelet-leader based Bayesian multivariate multifractal formalism. To that end, Section II recalls the key elements of (multivariate) multifractal analysis and details the key step of the Bayesian formulation. Section III describes the set of exchange rates studied here. Section IV compares the analysis of cross-temporal dynamics in forex market assessed by second-order statistics and classical linear correlations against the richer characterization permitted by multivariate multifractal analysis, in terms of co-burstiness in volatility and universal clock.

II. Bayesian Multivariate multifractal Analysis

A. Multivariate multifractal analysis

Theory. Multivariate multifractal analysis jointly quantifies the fluctuations along time of the pointwise regularities, com-

monly quantified by Hölder exponents $h_{X_r}(t) \geq 0$, for a set of signals $\boldsymbol{X}(t) = (X_1(t), \ldots, X_M(t)) \in \mathbb{R}^M$, $t \in \mathbb{R}$. The *M-variate multifractal spectrum* $\mathcal{D}(h_1, \ldots, h_M)$ of $\boldsymbol{X}$, defined as the collection of Hausdorff dimensions $\dim_H$ of the sets of points t with the same M-uplet of Hölder exponents $\boldsymbol{h} = (h_1, \ldots, h_M)$, provides a global and geometrical description of the temporal joint organization of these pointwise regularity fluctuations of $\boldsymbol{X}$. Interested readers are referred to [8]–[10], [15] for more detailed introductions.

Practice. It has been well documented that multifractal analysis can be efficiently conducted practically using wavelet leaders as relevant multiscale representations, see *e.g.*, [9], [10]. Let ψ denote the *mother wavelet*, a well time-frequency localized oscillating pattern, characterized by its number of vanishing moments N_ψ defined as $\forall n = 0, \ldots, N_\psi - 1$, $\int_{\mathbb{R}} t^n \psi(t) dt \equiv 0$ and $\int_{\mathbb{R}} t^{N_\psi} \psi(t) dt \neq 0$. The L^1 normalized discrete wavelet transform coefficients are defined by $d_X(j,k) = 2^{-j} \langle \psi(2^{-j} \cdot - k) | X(\cdot) \rangle$, see *e.g.*, [16]. The *wavelet leaders* of X are defined as $L_X(j,k) \triangleq \sup_{\lambda' \subset 3\lambda_{j,k}} |d_X(\lambda')|$, with $\lambda_{j,k} = [k2^j, (k+1)2^j)$ the dyadic interval of size 2^j, and $3\lambda_{j,k}$ the union of $\lambda_{j,k}$ with its 2 neighbors.

For simplicity, bivariate ($M = 2$) multifractal analysis only is presented here, extension to M-variate cases are straightforward [8]–[10]. Let $\boldsymbol{\ell_X}(j,k) \triangleq (\ln L_{X_1}(j,k), \ln L_{X_2}(j,k)) \in \mathbb{R}^2$ denote the vector of bivariate log-leaders at scale j, and the corresponding bivariate cumulants $C_{p_1p_2}(j)$, $p_1 + p_2 \geq 1$.

For large classes of multivariate multifractal processes, the $C_{p_1p_2}(j)$ evolve linearly across (the logarithm of the) scales 2^j, $C_{p_1p_2}(j) = c^0_{p_1p_2} + j\, c_{p_1p_2} \ln 2$, see *e.g.*, [17]. The coefficients of the scaling behaviors, $c_{p_1p_2}$ critically define an approximation of the bivariate multifractal spectrum:

$$\mathcal{D}(h_1, h_2) \approx 1 + \frac{c_{02} b}{2} \left(\frac{h_1 - c_{10}}{b} \right)^2 + \frac{c_{20} b}{2} \left(\frac{h_2 - c_{01}}{b} \right)^2 - c_{11} b \left(\frac{h_1 - c_{10}}{b} \right) \left(\frac{h_2 - c_{01}}{b} \right), \quad (1)$$

where c_{20}, $c_{02} < 0$, $b \triangleq c_{20}c_{02} - c_{11}^2 \geq 0$ [18].

Multifractal correlation. While (c_{10}, c_{20}) (resp. (c_{01}, c_{02})) characterize the multifractal properties of X_1 (resp. X_2), c_{11} assesses cross-multifractality between X_1 and X_2, hence cross-temporal dynamics not already captured by the classical inter-correlation function. Mimicking the classical linear (Pearson) correlation coefficient, this leads to define

$$\rho^{MF} \triangleq -\frac{c_{11}}{\sqrt{c_{20}c_{02}}}, \quad (2)$$

referred to as *multifractal correlation*, with a slight yet assumed abuse, as this is quantifying cross-temporal dynamics beyond second-order.

B. Bayesian estimation for joint multifractality parameters

Estimation. Efficiently estimating parameters (c_{20}, c_{02}, c_{11}) constitutes a major challenge in the practical use of (multivariate) multifractal analysis. Classically, estimation relies on linear regressions of sample cumulants across scale j and often suffer from large estimation variance, notably for small sample size. Recently, a Bayesian estimation framework was developed with much improved estimation performance [13], [14]. Essentially, it relies on the assumption that the centered version of the log-leaders $\ell_X(j,k)$, denoted $\boldsymbol{l_X}(j,k) = [l_{X_1}(j,k), l_{X_2}(j,k)]^T$, is well-modeled as a Gaussian random vector with point covariance matrix parameterized by two 2×2 positive definite real-valued matrices $\boldsymbol{\Sigma_1}$ and $\boldsymbol{\Sigma}_2$, *i.e.*, $\boldsymbol{l_X}(j,k) \sim \mathcal{N}(\boldsymbol{0}, \boldsymbol{\Sigma_1} \ln 2^{-j} + \boldsymbol{\Sigma}_2)$, where $\boldsymbol{\Sigma_1} \triangleq -\begin{pmatrix} c_{20} & c_{11} \\ c_{11} & c_{02} \end{pmatrix}$ contains the parameters of interest.

Whittle approximation and data augmentation. To simplify the inference model, a Whittle approximation permits to diagonalize the known and fixed temporal covariance and to factorize the joint distribution of the Fourier coefficients $\boldsymbol{z}_j = \mathcal{F}_{I_j}(\boldsymbol{l_X}(j,\cdot))$ [19], [20]. Operator $\mathcal{F}_{I_j}(\cdot)$ computes and vectorizes the discrete Fourier coefficients contained in $I_j = [\![-\lceil \sqrt{n_j}/2 \rceil + 1, \lceil \sqrt{n_j}/2 \rceil]\!] \setminus \{0\}$ ($[\![a_1, a_2]\!]$ denotes the set of integers ranging from a_1 to a_2) with frequencies $\left\{ \omega_m = 2\pi m / \sqrt{n_j} \right\}_{m \in I_j}$ and $\lceil \cdot \rceil$ denotes the next largest integer. Data augmentation is then used to introduce a complex-valued vector of latent variables $\boldsymbol{u} \in \mathbb{C}^{2M}$, which leads to the augmented likelihood, $p(\boldsymbol{z}, \boldsymbol{u} \mid \boldsymbol{\Sigma}_1, \boldsymbol{\Sigma}_2) \propto p(\boldsymbol{z} \mid \boldsymbol{u}, \boldsymbol{\Sigma}_1) p(\boldsymbol{u} \mid \boldsymbol{\Sigma}_2)$. The vectors $\boldsymbol{z}$ and $\boldsymbol{u}$ have conditional distributions $\boldsymbol{z} \mid \boldsymbol{u}, \boldsymbol{\Sigma}_1 \sim \mathcal{CN}(\boldsymbol{u}, \boldsymbol{\Sigma}_1 \otimes \boldsymbol{G}_1)$ and $\boldsymbol{u} \mid \boldsymbol{\Sigma}_2 \sim \mathcal{CN}(\boldsymbol{0}, \boldsymbol{\Sigma}_2 \otimes \boldsymbol{G}_2)$, where $\mathcal{CN}$ denotes the complex Gaussian distribution. The matrices $\boldsymbol{G}_1$ and $\boldsymbol{G}_2$ are deterministic diagonal matrices that subsume the covariance model in time. Thus, $p(\boldsymbol{z}, \boldsymbol{u} \mid \boldsymbol{\Sigma}_1, \boldsymbol{\Sigma}_2)$ consists of the product of complex Gaussian distributions with covariance matrices $\boldsymbol{\Sigma}_1$ and $\boldsymbol{\Sigma}_2$.

Prior. The scaled inverse Wishart (SIW) prior uses a factorization $\boldsymbol{\Sigma}_i \triangleq \boldsymbol{\Delta}_i \boldsymbol{Q}_i \boldsymbol{\Delta}_i$ with independent random matrices $\boldsymbol{Q}_i$ and $\boldsymbol{\Delta}_i$ to decouple estimation for the diagonal and off-diagonal elements of $\boldsymbol{\Sigma}_i$ [21]. Specifically, $\boldsymbol{Q}_i \sim \mathcal{IW}(\nu_i, \boldsymbol{\Lambda}_i)$, and $\boldsymbol{\Delta}_i$ is a diagonal matrix with independent diagonal elements $\delta_{ir} = [\boldsymbol{\Delta}_i]_{rr}$ and $\delta_{ir} \sim \mathcal{LN}(\beta_{ir}, \alpha_{ir}^2)$, with $\mathcal{LN}$ the log-normal distribution: $p(\boldsymbol{\Sigma}_i) = p(\boldsymbol{Q}_i) p(\delta_{i1}) p(\delta_{i2})$, $i \in \{1, 2\}$.

Posterior. Using Bayes' rule, the posterior distribution for $\boldsymbol{\Sigma}_1$, $\boldsymbol{\Sigma}_2$ and the latent vector $\boldsymbol{u}$, $p(\boldsymbol{\Sigma}_1, \boldsymbol{\Sigma}_2, \boldsymbol{u} \mid \boldsymbol{z}) \propto p(\boldsymbol{z}, \boldsymbol{u}, \mid \boldsymbol{\Sigma}_1, \boldsymbol{\Sigma}_2) p(\boldsymbol{\Sigma}_1) p(\boldsymbol{\Sigma}_2)$, can be used to define the marginal MMSE estimator $\widehat{\boldsymbol{\Sigma}}_i^{\text{MMSE}} \triangleq \mathbb{E}[\boldsymbol{\Sigma}_i \mid \boldsymbol{z}, \boldsymbol{u}]$, an approximation of which is computed using Monte Carlo Markov chains.

Gibbs sampler. Samples $\{\boldsymbol{\Sigma}_1^{(\lambda)}, \boldsymbol{\Sigma}_2^{(\lambda)}, \boldsymbol{u}^{(\lambda)}\}_{\lambda=1}^{N_{\text{mc}}}$ are successively drawn from the conditional distributions:

$$\begin{aligned} \boldsymbol{Q}_i \mid \boldsymbol{\Delta}_i, \boldsymbol{z}, \boldsymbol{u} &\sim \mathcal{IW}(\nu_i + 2M, \boldsymbol{\Lambda}_i + \boldsymbol{\Delta}_i^{-1} \tilde{\boldsymbol{\Phi}}_i \boldsymbol{\Delta}_i^{-1}) \quad (3) \\ \delta_{ir} &\sim f(\delta_{ir}) = p(\delta_{ir} \mid \boldsymbol{Q}_i, \{\delta_{ir'}\}_{r' \neq r}, \boldsymbol{z}, \boldsymbol{u}) \quad (4) \\ & \quad \boldsymbol{\Sigma}_i \triangleq \boldsymbol{\Delta}_i \boldsymbol{Q}_i \boldsymbol{\Delta}_i \\ \boldsymbol{u} \mid \boldsymbol{z}, \boldsymbol{\Sigma}_1, \boldsymbol{\Sigma}_2 &\sim \mathcal{CN}(\tilde{\boldsymbol{\mu}}, \tilde{\boldsymbol{\Sigma}}), \quad (5) \end{aligned}$$

with $\tilde{\boldsymbol{\Phi}}_1 = 2\,\mathrm{Re}(\sum_{s=1}^M (\boldsymbol{z}_s - \boldsymbol{u}_s)(\boldsymbol{z}_s - \boldsymbol{u}_s)^H g_{1s}^{-1})$ and $\tilde{\boldsymbol{\Phi}}_2 = 2\,\mathrm{Re}(\sum_{s=1}^M \boldsymbol{u}_s \boldsymbol{u}_s^H g_{2s}^{-1})$, $g_{is} = [\boldsymbol{G}_i]_{ss}$, $i = \{1, 2\}$. $\tilde{\boldsymbol{\Sigma}}$ is a block diagonal matrix whose s^{th} block is $\tilde{\boldsymbol{\Sigma}}_s = \left[(g_{1s}\boldsymbol{\Sigma}_1)^{-1} + (g_{2s}\boldsymbol{\Sigma}_2)^{-1} \right]^{-1}$, and $\tilde{\boldsymbol{\mu}}_s = \tilde{\boldsymbol{\Sigma}}_s (g_{1s}\boldsymbol{\Sigma}_1)^{-1} \boldsymbol{z}_s$. $f(\delta_{ir})$ is not a standard distribution and is sampled using the

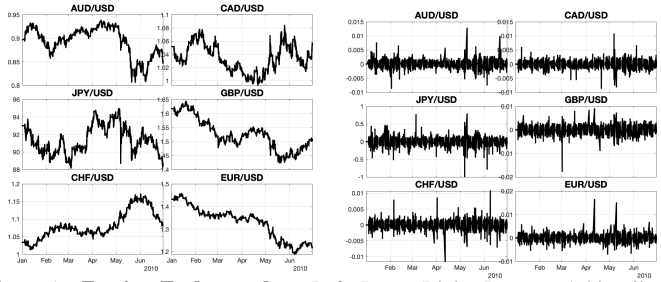

Figure 1. **Foreign Exchange data.** Left: Rates; Right: Returns. Arbitrarily chosen 6-month window.

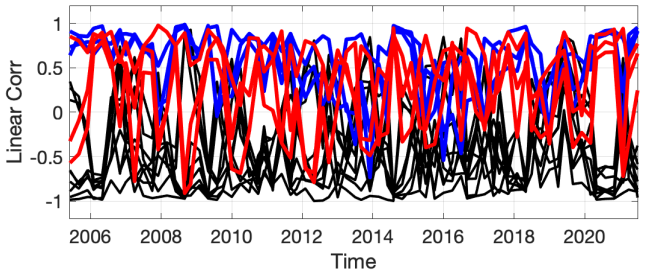

Figure 2. **Time evolution of the linear (Pearson) correlation Coefficients.** Red and blue lines correspond to intra-group correlations, black line to inter-groups correlations. See text for details.

log-conditional distribution:

$$\begin{aligned}\ln(f(\delta_{ir})) = &-(2M+1)\ln(\delta_{ir}) - [\boldsymbol{Q}_i^{-1}]_{rr}[\tilde{\boldsymbol{\Phi}}_i]_{rr}(2\delta_{ir}^2)^{-1} \\ &- \delta_{ir}^{-1}\delta_{ir'}^{-1}[\boldsymbol{Q}_i^{-1}]_{rr'}[\tilde{\boldsymbol{\Phi}}_i]_{rr'} \\ &- (\ln(\delta_{ir}) - \beta_{ir})^2/(2\alpha_{ir}^2) + \text{constant}.\end{aligned}$$

Metropolis-Hastings random walks are used for sampling each δ_{ir} [21]. Finally, the MMSE estimator $\widehat{\boldsymbol{\Sigma}}_i^{\text{MMSE}}$ is approximated as the average, after burn-in, of $\{\boldsymbol{\Sigma}_i^{(\lambda)}\}_{\lambda=N_{\text{bi}}+1}^{N_{\text{mc}}}$.

III. Foreign Exchange Rates

The intraday ($T_s = 5$ min sampling period) exchange rates used in this longitudinal study range from March 2005 to November 2021 and comprises the Australian Dollar (AUD), Canadian Dollar (CAD), Japanese Yen (JPY), Swiss Franc (CHF), Euro (EUR) and British Pound (GBP), against the US Dollar (USD). Bivariate analysis for the pair of rates *XXX/USD* and *YYY/USD* will be simply referred to as *XXX-YYY*. Rates and returns (increments) for these six couples of currencies and for the chosen period are shown in Fig. 1

IV. Cross-temporal dynamics longitudinal study

A. Longitudinal analysis set-up

Cross-temporal dynamics and multifractal parameters are estimated within 6-month sliding windows, with 3-month time shift. Wavelet analysis is performed using a least asymmetric Daubechies wavelet with $N_\psi = 3$ [22]. Bayesian estimation is performed using SIW prior, with $\Delta_i = I$, $\nu_i = 4$, and $(\beta_{ir}, \alpha_{ir}^2) = (0.1, 1)$. Gibbs samplers produce $N_{mc} = 2000$ samples, after a burn-in of $N_{bi} = 500$ samples.

B. Linear Correlation

Pearson correlation coefficients. Naturally, the study of (cross-)temporal dynamics must start with the second-order statistics inter- and autocorrelation functions. It has been abundantly documented that, for most asset return time series, these functions are estimated close to 0 beyond lag 0 [23], clearly indicating that second-order statistics based analysis only suggest multivariate White noise type (cross)-temporal dynamics. For instance, this was thoroughly demonstrated and quantified in [11] for a global period of two years of exchange rates using wavelet based multiscale statistics. The same analysis (not reported here for space reasons) yield identical conclusions for each of the 6-month windows analyzed here.

Second-order statistics cross-temporal dynamics analysis thus boils down to computing (Pearson) correlation coefficient ρ between pairs of exchange rates, for each time window. These ρs, for each of the $15 = 6\times5/2$ pairs of exchange rates, are reported as functions of time, in Fig. 2. Disregarding colors for the time being, Fig. 2 shows first that Pearson correlation coefficients vary widely and rapidly along time and cover the full accessible range of values $(-1, 1)$.

Multidimensional scaling representations. To better understand the evolution of the dependence structure among exchange rates, the matrix of ρs is transformed, independently for each time window, into an affinity Matrix A, with entries $A_{m,m'} = \exp(-(1-\rho_{m,m'})^2)$. Then, standard *Kruskal's normalized stress multidimensional scaling* (2D) representations [24] are created and illustrated in Fig. 3. For the full 17-year period (Fig. 3, top left), such a representation shows that EUR, GBP and AUD are consistently close, while CHF, CAD and JPY tend to form another group, though less close. The presence of AUD in the first cluster reflects the anchoring of most currencies to the USD rather than a direct relationship between them [25]. In Fig. 2, the red (blue, resp.) lines corresponds to ρs for all pairs among the first (second, resp.) cluster, while black lines reports ρs for pairs of rates mixing both groups. It shows intra-group correlations are essentially positive while inter-group correlations are mostly negative. This is thus indicating that groups are mostly gathering currencies showing same variations with respect to the USD. Fig. 3 also shows multidimensional scaling plots for three different 6-month windows: During the European sovereign debt crisis (2010-2012, Fig. 3 top right); the period when the Swiss National Bank (SNB) set a minimum exchange rate of CHF vs. EUR (2012-2014, Fig. 3 bottom left); the period including the Brexit and Covid-19 pandemics (2016-2021, Fig. 3 bottom left). The GBP's departure from the main cluster following Brexit is very clear. The position of the CHF with respect to the main cluster is quite stable, even during the SNB's active exchange rate policy, while the positions of the CAD and the JPY are more wandering. These observations are fully consistent with the existence of local factors influencing the dynamics of exchange rate movements [26]–[28].

Beyond linear correlations. All together, Fig. 3 show that second-order based assessment of dependence in exchange

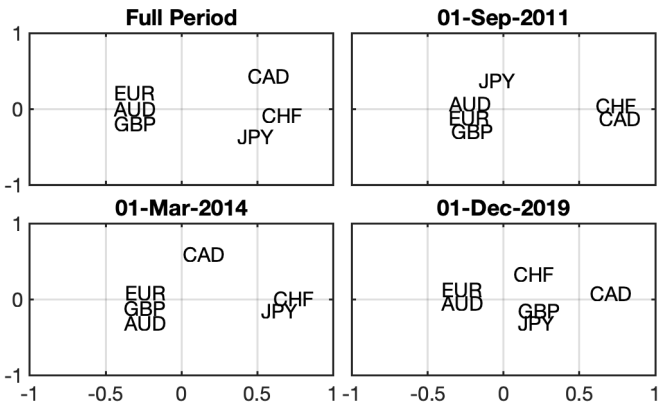

Figure 3. **Similarities in cross-temporal dynamics assessed by linear correlations** by multidimensional scaling representations, for the 17-year period (top left) and three chosen 6-month windows.

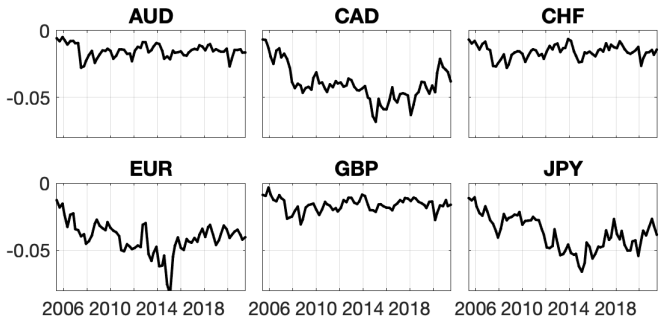

Figure 4. **Time evolution of the multifractality parameter** c_{20}**.**

rates is extremely volatile and mostly captures a global and static co-movement of currencies with USD, thus calling for better assessment of cross-temporal dynamics, as permitted by multifractal analysis.

C. Multifractal Correlation

Scaling range. The (Bayesian) multifractal analysis tools applied here to each 6-month time window indicate, quite remarkably for real-wold data, scalefree temporal dynamics for scales ranging from $2^{j_1} = 8$ to $2^{j_2} = 512$, that is, from $\simeq 40$ min to $\simeq 3$ days, in agreement with the literature, see *e.g.*, [11]. This range of octaves is thus used to estimate c_{10} and c_{20} for the 6 exchange rates, and c_{11} and thus ρ^{MF} for the 15 pairs, independently in each time windows.

Univariate multifractal analysis. Parameters c_{10} are estimated consistently along time and for all currencies around 0.5, confirming a global multivariate white noise temporal dynamics. However, c_{20} departs significantly from 0, consistently along time and for each exchange rate independently (Fig. 4), confirming a solid and consistent multifractality in each exchange rate time series, and thus rich temporal dynamics in terms of local transient structures occurring in well-organized time patterns, often related to volatility burstiness [29]. This is thus motivating the use of bivariate multifractal analysis to assess rich cross-temporal dynamics beyond what can actually be captured by second-order statistics.

Bivariate multifractal analysis. Fig. 5 reports the evolution along time of ρ^{MF} for the 15 pairs of exchange rates. Strikingly, it shows, disregarding colors for the time being, that multifractal correlations are, for all time windows and all pairs, only always significantly positive. This indicates that multifractal correlation is capturing (all-order statistics) dependencies in temporal dynamics of exchange rates that totally differ from those assessed by second-order only, both as functions of time and cross-section wise. Essentially, the high positive level of ρ^{MF} suggest that all 6 exchange rates share closely related temporal dynamics features. Notably, burstiness and local transient structures occur for all currencies with same structured temporal patterns, and jointly. This is thus as if a universal clock was controlling the entire forex market, in other words, as if the same process $A(t)$ was used to subordinate 6 different Brownian motions $B_m(t)$.

Further, multidimensional scaling representations, computed replacing the matrix Pearson linear correlations ρ by that of multifractal correlations ρ^{MF}, are reported in Fig. 6, for the global 17-year period and the same three 6-month periods. It indicates that the temporal dynamics of western country currency exchange rates (EUR, GBP, CHF and CAD) are extremely intertwined, and this consistently along time periods. The temporal dynamics of the Asia-Pacific country exchange rates are less coordinated with those of western countries, in accordance with the existence of second order local factors driving the volatility of exchange rates [30]. This is illustrated in complementary manner in Fig. 5 with red (resp. blue) curves for pairs involving JPY (resp. AUD), showing slightly lower multifractal correlations. Interestingly, Fig. 6 shows that, both during the European debts crisis (top left) and CHF/EUR ceiling exchange rate period (bottom right), CHF exhibits temporal dynamics in terms of volatility burstiness, closely related to that of EUR and GBP, and this despite having negative Pearson (linear) correlation. This means that despite having opposite sign variations with respect to USD, EUR and GBP, CHF undergoes actually the same sporadic increases and bursts of volatility. CAD, that showed opposite variations to USD compared to EUR or GBP, however also share closely related burstiness in volatility. The converse is observed for AUD, that showed same variations to USD compared to EUR or GBP, yet with less tightly related volatility burstiness. Finally and interestingly, Fig. 6 (bottom right) shows that during the most recent period the cross-sectional dependencies assessed by multifractal correlations are far less shuffled then that quantified by linear correlation. All together, multifractal correlations between JPY (or AUD) and the western currencies are slightly lower after 2013, compared to before, potentially suggesting a slightly decreasing integration of financial activities worldwide.

V. Conclusions and perspectives

In conclusions, the present work showed that multivariate multifractal analysis permits to assess cross-temporal dynamics by quantifying the jointly organized occurrence of local transient structures, or coburstiness, beyond what is already

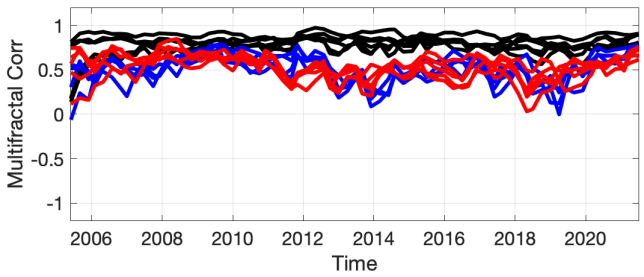

Figure 5. **Time evolution of multifractal correlations ρ^{MF}.** red and blue lines correspond to pairs of forex rates involving respectively JPY and AUD. See text for details.

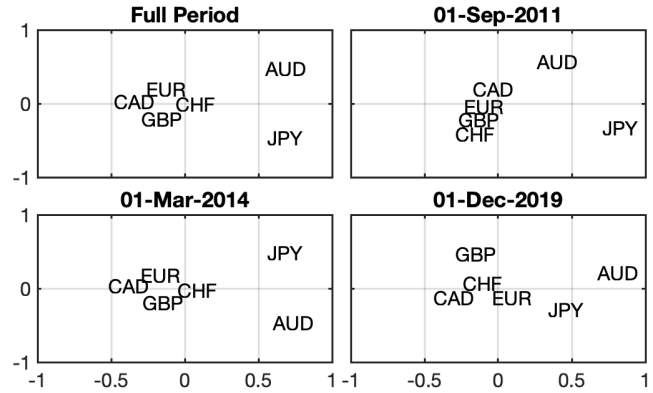

Figure 6. **Similarities in cross-temporal dynamics assessed by multifractal correlations** by multidimensional scaling representations, for the 17-year period (top left) and three chosen 6-month windows.

captured by second-order statistics global dependencies. Multivariate multifractal analysis thus complements and enriches with novel information cross-correlation analysis. Applied to forex market to perform a longitudinal study, the present work showed that multifractal correlations indicate integrated and joint co-burstiness worldwide, with limited impact of significant international crises on the cross-sectional dependence structure, while linear correlations essentially split currencies in terms of groups with same global covariations against the USD. The high multifractal correlations are also reminiscent of a worldwide synchronizing clock that drives the forex market.

This work will be extended in several respects: Multivariate beyond bivariate analyses will be explored on real world data ; Other categories of financial assets, such as stock prices or stock market indices, will be investigated. In an effort toward reproducible research and open science, Matlab codes implementing (Bayesian) multivariate multifractal analysis are made publicly available[1].

References

[1] Y. Malevergne and D. Sornette, *Extreme Financial Risks: From Dependence to Risk Management*. Springer, 2006.

[2] B. J. Christensen and M. Ø. Nielsen, "The effect of long memory in volatility on stock market fluctuations," *The Review of Economics and Statistics*, vol. 89, no. 4, pp. 684–700, 2007.

[3] B. B. Mandelbrot, *Fractals and scaling in finance: Discontinuity, concentration, risk. Selecta volume E.* Springer, 2013.

[4] T. Di Matteo, T. Aste, and M. M. Dacorogna, "Long-term memories of developed and emerging markets: Using the scaling analysis to characterize their stage of development," *Journal of banking & finance*, vol. 29, no. 4, pp. 827–851, 2005.

[5] L. E. Calvet and A. J. Fisher, *Multifractal volatility: theory, forecasting, and pricing*. Academic Press, 2008.

[6] E. Bacry, A. Kozhemyak, and J. Muzy, "Multifractal models for asset prices," *Encyclopedia of quantitative finance, Wiley*, 2010.

[7] T. Lux and M. Segnon, "Multifractal models in finance: Their origin, properties and applications," 2016.

[8] C. Meneveau, K. Sreenivasan, P. Kailasnath, and M. Fan, "Joint multifractal measures - theory and applications to turbulence," *Physical Review A*, vol. 41, no. 2, pp. 894–913, January 1990.

[9] S. Jaffard, S. Seuret, H. Wendt, R. Leonarduzzi, S. Roux, and P. Abry, "Multivariate multifractal analysis," *Applied and Computational Harmonic Analysis*, vol. 46, no. 3, pp. 653–663, 2019.

[10] S. Jaffard, S. Seuret, H. Wendt, R. Leonarduzzi, and P. Abry, "Multifractal formalisms for multivariate analysis," *Proc. Royal Society A*, vol. 475, no. 2229, 2019.

[11] P. Abry, Y. Malevergne, H. Wendt, S. Jaffard, M. Senneret, and L. Jaffrès, "Foreign exchange multivariate multifractal analysis," in *Proc. European Signal Process. Conf.* IEEE, 2022, pp. 2121–2125.

[12] S. Combrexelle, H. Wendt, N. Dobigeon, J.-Y. Tourneret, S. McLaughlin, and P. Abry, "Bayesian estimation of the multifractality parameter for image texture using a whittle approximation," *IEEE T. Image Proces.*, vol. 24, no. 8, pp. 2540–2551, 2015.

[13] L. Leon, H. Wendt, J.-Y. Tourneret, and P. Abry, "Bayesian estimation for the parameters of the bivariate multifractal spectrum," in *Proc. European Signal Process. Conf.*

[14] ——, "A bayesian framework for multivariate multifractal analysis," *IEEE T. Signal Proces.*, vol. 70, pp. 3663–3675, 2022.

[15] S. Jaffard, "Wavelet techniques in multifractal analysis," in *Fractal Geometry and Applications: A Jubilee of Benoît Mandelbrot, M. Lapidus and M. van Frankenhuijsen, Eds., Proc. Symposia in Pure Mathematics*, vol. 72(2). AMS, 2004, pp. 91–152.

[16] S. Mallat, *A wavelet tour of signal processing*, 2nd ed. San Diego, CA: Academic Press, 2009.

[17] B. Castaing, Y. Gagne, and M. Marchand, "Log-similarity for turbulent flows," *Physica D*, vol. 68, no. 3-4, pp. 387–400, 1993.

[18] R. Leonarduzzi, P. Abry, S. G. Roux, H. Wendt, S. Jaffard, and S. Seuret, "Multifractal characterization for bivariate data," in *Proc. European Signal Process. Conf.*, 2018.

[19] P. Whittle, "Estimation and information in stationary time series," *Ark. Mat.*, vol. 2, no. 5, pp. 423–434, 1953.

[20] A. M. Sykulski, S. C. Olhede, J. M. Lilly, and J. J. Early, "Frequency-domain stochastic modeling of stationary bivariate or complex-valued signals," *IEEE T. Signal Process.*, vol. 65, no. 12, pp. 3136–3151, 2017.

[21] A. J. O'Malley and A. M. Zaslavsky, "Domain-level covariance analysis for multilevel survey data with structured nonresponse," *J. of the Am. Stat. Assoc.*, vol. 103, no. 484, pp. 1405–1418, 2008.

[22] S. Mallat, *A Wavelet Tour of Signal Processing*. San Diego, CA: Academic Press, 1998.

[23] J. Y. Campbell, A. W. Lo, and A. C. MacKinlay, *The Econometrics of Financial Markets*. Princeton University Press, 1997.

[24] A. Mead, "Review of the development of multidimensional scaling methods," *Journal of the Royal Statistical Society: Series D (The Statistician)*, vol. 41, no. 1, pp. 27–39, 1992.

[25] E. Ilzetzki, C. M. Reinhart, and K. S. Rogoff, "Rethinking exchange rate regimes," in *Handbook of international economics*. Elsevier, 2022, vol. 6, pp. 91–145.

[26] R. Chiappini and D. Lahet, "Exchange rate movements in emerging economies-global vs regional factors in asia," *China Economic Review*, vol. 60, p. 101386, 2020.

[27] K. Jaworski, "Forecasting exchange rates for central and eastern european currencies using country-specific factors," *Journal of Forecasting*, vol. 40, no. 6, pp. 977–999, 2021.

[28] Y. E. Ergemen and C. V. Rodríguez-Caballero, "Estimation of a dynamic multi-level factor model with possible long-range dependence," *International Journal of Forecasting*, vol. 39, no. 1, pp. 405–430, 2023.

[29] R. Cont, "Empirical properties of asset returns: stylized facts and statistical issues," *Quantitative finance*, vol. 1, no. 2, pp. 223–236, 2001.

[30] M. Caporin, C. V. Rodríguez-Caballero, and E. Ruiz, "The factor structure of exchange rates volatility: global and intermittent factors," *Empirical Economics*, pp. 1–15, 2024.

[1] https://www.irit.fr/~Herwig.Wendt/software.html